

# MATERIAL PROPERTIES OF ZINC PHTHALOCYANINE FROM FA SOLUTION AND APPLICATION IN ORGANIC SOLAR CELLS

<sup>1</sup>TAMARA POTLOG, <sup>2</sup>VADIM FURTUNA, <sup>3</sup>CORNEL ROTARU, <sup>4</sup>ROMAN RUSNAC, <sup>5</sup>STEFAN ROBU, <sup>6</sup>TOMOAKI MASUZAWA, <sup>7</sup>HIDENORI MIMURA

<sup>1,2,3</sup>Department of Physics and Engineering, Moldova State University, Chisinau, MD-2009, Moldova  
<sup>4,5</sup>Faculty of Chemistry and Chemical Technology, Moldova State University, Chisinau, MD-2009, Moldova  
<sup>6,7</sup>Research Institute of Electronics, Shizuoka University, Hamamatsu, 432-8011, Japan  
E-mail: <sup>1</sup>tpotlog@gmail.com, <sup>7</sup>mimura.hidenori@shizuoka.ac.jp

**Abstract** - This paper presents for a first time a solution-processable ZnPc thin films from formic acid (FA) solution by drop casting method and the photovoltaic parameters of the Organic Solar Cells (OPV) based on ZnPc-diode Schottky. Structural and optical properties of ZnPc thin films were investigated by X-ray diffraction (XRD), Fourier transform infrared spectroscopy (FTIR) and UV-VIS spectroscopy. XRD analysis shows phase transformation of the alpha-beta phases of ZnPc thin films to beta phase due to the annealing in H<sub>2</sub> atmosphere at 400°C for 30 min. FTIR analysis shows that the formate ion (HCOO<sup>-</sup>) is attached to Zn(II)Pc. Further on, ITO/PEDOT: PSS/ZnPc(I<sub>2</sub>)/Al Schottky photovoltaic devices with efficiency of 0.3 % were prepared and their characteristics 'enhancement is discussed. The values for the open circuit voltage (1.03 V) and the current density (8.2 μA/cm<sup>2</sup>) are higher than in the case of Schottky diode devices obtained by thermal vacuum evaporation.

**Keywords** - Drop Casting Method, Zinc Phthalocyanine, Formic Acid, Thin Film, Organic Solar Cells.

## I. INTRODUCTION

Zinc phthalocyanine (ZnPc) is a particularly attractive sub-class of Pcs given the elemental abundance, very low toxicity levels, *p*-type conductivity [1], low band gap (~ 1.8 eV) well-matched to the incident solar spectrum [2] and light [3], thermal, and chemical resistances. The lengths of the C-N bonds in the isoindole fragments of the macro ring of ZnPc oscillate between 1.73 – 1.38 Å and are very close by length to that of all 24 bonds in benzene fragments (1.38 – 1.43 Å). The lengths of the C-N bonds with nitrogen bridge atoms is within the limits 1.31-1.34 Å. At the same time, the lengths of all eight C-C bonds between the macro cycle and the benzene rings are substantially larger and have the values of 1.46 - 1.49 Å, meaning it approaches to the length of the σ bond (1.54 Å) [4]. This indicates the fact that the conjugation between the π-electron systems of the macrocycle and of the four benzene rings is not very high, meaning that in the molecule there are the quasi-autonomous aromatic systems of the four benzene rings and of the internal macrocycle (consisting of 16 atoms) in which the number of own π electrons (eighteen) also correspond to Hückel's rule [5]. Thanks to this structure, the ZnPc compound allows the electrical transport and interacts with light; therefore, it is a material with important applications in optoelectronics. Recently, ZnPc has drawn considerable attention because of employing as hole-transporting material in mixed-ion [FAPbI<sub>3</sub>]<sub>0.85</sub>[MAPbBr<sub>3</sub>]<sub>0.15</sub> perovskite solar cells, that reaching the highest power conversion efficiency (PCE), 17.5% so far for phthalocyanines [6]. The unsubstituted metal phthalocyanines have very low solubility in the majority of the solvents [7,

8], therefore many studies focused on the formation of substituted complexes to improve solubility in the manufacturing process. Unfortunately, most of the substituted phthalocyanines are not as stable as the unsubstituted compounds, and their electronic properties differ from those of the unsubstituted phthalocyanines [9, 10]. From the available literature and to the knowledge of the authors not much investigations have been carried out on the physical properties of solution processable zinc phthalocyanine thin films from solution, therefore more detailed investigations are needed before going in for an all-organic optoelectronic device. In this paper, we are reporting morphology, structure, optical properties of solution-processable ZnPc thin films from FA solution and photovoltaic parameters of the Organic Solar Cells (OPV) based on the diode Schottky.

## II. SYNTHESIS OF ZnPc THIN FILMS

Commercially available zinc phthalocyanine (ZnPc) powder (98% purity) was purchased from Sigma Aldrich and was used without further purification. The formic acid (FA) (99% purity) and dimethylformamide (DMF) (99.8% purity) also, purchased from Sigma Aldrich were selected as the solvents for ZnPc. The ZnPc powder was added to the solvents of 60%, 80% and 98% concentrations of formic acid (FA), and the solutions were sonicated for 5 min using an ultrasonic cleaner. In the solution with lower 60% FA concentration the aggregation of undissolved ZnPc was observed. The solution was prepared by dissolving the ZnPc at a concentration of 1 mg/ml into a mixture of DMF and FA solvents. The reaction is accelerated by increasing the amount of

formic acid added and the temperature. The solutions were left to stand for 48 h at room temperature and checked for the precipitation to determine the solubility of the ZnPc. We used for our solubility studies the absorption intensity of the Q-band as a measure for the concentration of the solution. In cases in which more than one intensive Q-band exists (Q-band splitting), we took only the molar absorption coefficient of the stronger transition as a measure for the solubility. The molar absorption coefficient of the Q band is in the range of  $2.5-3 \cdot 10^5 \text{ L} \cdot \text{mol}^{-1} \cdot \text{cm}^{-1}$  for the ZnPc thin films obtained from lower 60% FA solution. After that, the obtained solution was doped with iodine and again sonicated. The obtained solution was subsequently used for the deposition of ZnPc thin films on glass and ITO substrates, by the drop casting method.

### III. EXPERIMENTAL DETAILS

The structure of the films was analyzed by X-ray Bruker D8 advanced diffractometer (using  $\text{CuK}_\alpha$  radiation with  $\lambda=1.5406 \text{ \AA}$ ). The crystallite size (D) was calculated from the XRD patterns according to the well-known Scherer equation:

$$D = \frac{0.9 \lambda}{\beta \cos \theta},$$

where  $\beta$  is the full-width at half-maximum (FWHM) peak for a Bragg angle  $\theta$ , and  $\lambda$  is the wavelength of the X-ray radiation. FTIR spectrometers (Bruker IFS 66 v/S & Vertex 80 V) were used for the measurements of transmittance spectra in a frequency range between  $400 \text{ cm}^{-1}$  and  $4000 \text{ cm}^{-1}$ . All the transmittance measurements were carried out with a resolution of  $4 \text{ cm}^{-1}$  and a sample scan time of 1000 scans. The optical absorbance data was measured by JASCO V-670 spectrophotometer over the wavelength range of 350 nm to 900 nm. The measurements are made on films deposited on glass substrates with varying thickness.

### IV. RESULTS AND DISCUSSION

#### 4.1 Morphology and Structural Studies

ZnPc films of various thicknesses, ranging from 2.1  $\mu\text{m}$  (1 volume) to 8.0  $\mu\text{m}$  (4 volumes) of FA solutions have been prepared using the drop casting method. In Fig. 1a shown the SEM plane view of a ZnPc thin film obtained from one volume (2.1  $\mu\text{m}$ ) and four volume (8  $\mu\text{m}$ ) of solutions. The SEM micrographs indicate a smooth surface with a crystalline nature of the synthesized thin films. The surface of ZnPc thin film obtained from one volume of solution shows smaller grains at the bottom than that of ZnPc thin film obtained from four volumes of solution. Figure 2 shows the SEM cross section images of ZnPc thin films obtained from one volume and four volumes of solution on the glass/ITO/PEDOT:PSS substrates. The thickness is

observed to be enough uniform and reach the value of 2.0...2.1  $\mu\text{m}$  for one volume and 8  $\mu\text{m}$  for 4 volumes of solution. In addition, it has seen a not good adhesion for ZnPc thin film obtained from one volume of solution to the PEDOT:PSS film.

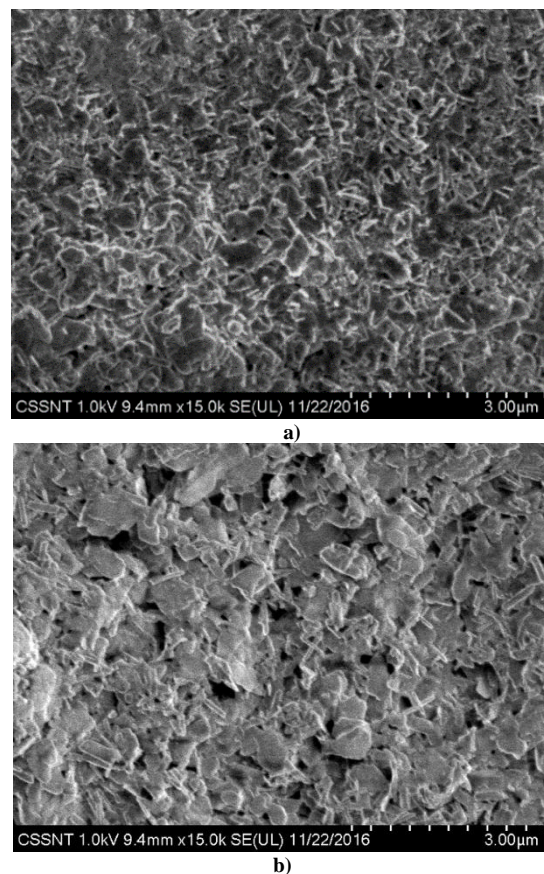


Figure 1: SEM micrograph of a drop casted ZnPc films synthesized from one (a) and four volumes of 98% FA solution at  $T=300 \text{ K}$  (b).

The X-ray diffractograms of the ZnPc films deposited from FA solution with different concentrations are presented in Figure 3. As one can see the XRD patterns of as-synthesized ZnPc thin films regardless of thickness exhibit polycrystalline structure and depend on the FA concentration. The XRD spectra of ZnPc thin films deposited from 98% FA solution display peaks situated at  $5.62^\circ$ ,  $7.99^\circ$  and  $16.67^\circ$  in comparison with that films deposited from 60% and 80% FA solution. In this case, according to well-known mechanism of dehydrogenation and dehydration of formic acid over zinc phthalocyanine [11], can be concluded that formic acid higher concentration interacts with ZnPc, dissociating to a formate ion,  $\text{HCOO}^-$ , and a proton, as is demonstrated in FTIR spectra. The FA is absorbed into the ZnPc to form metal formate and water, and the subsequent decomposition proceeds over the formate surface. The XRD patterns of ZnPc thin films synthesized on glass substrates from different volumes of 98% FA solution (different film thicknesses) are shown in Figure 4. The XRD patterns exhibit polycrystalline structure with the

major diffraction peak broadening at  $2\theta = 6.96^\circ$  and strong peakoverlapping reflections at  $2\theta=7.5^\circ, 8.03^\circ$  because of relatively complicated crystal structures. From Figure, it is observed that the intensity of the predominant peak increased with increasing film thicknesses.

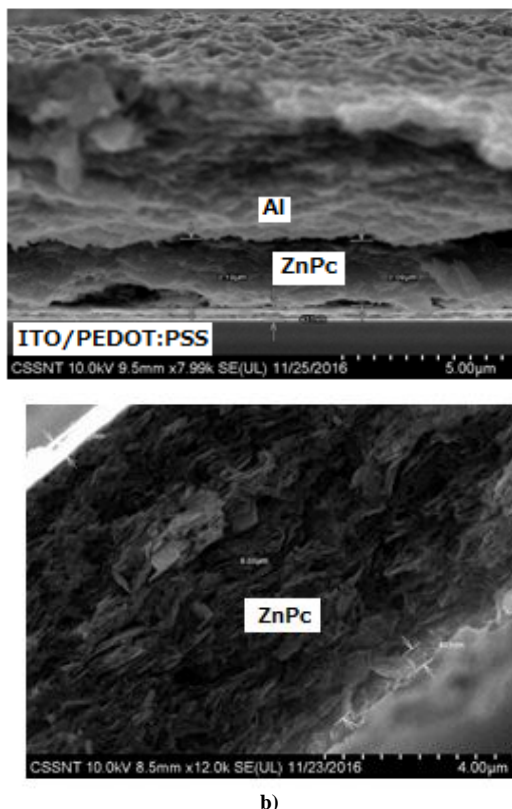


Figure 2: The SEM cross-section images of a drop casted ZnPc films synthesized from one (a) and four volumes of 98% FA solution at  $T = 300\text{ K}$  (b).

The shift of the reflection position from  $2\theta = 6.73^\circ$  for 2,1  $\mu\text{m}$  thick ZnPc layer to  $2\theta = 6.96^\circ$  for the 8,0  $\mu\text{m}$  thick layer results in slightly lattice deformation. Also, along with the predominant peak broadening in the ZnPc layers of 2,1  $\mu\text{m}$ , 4.0  $\mu\text{m}$  and 6.2  $\mu\text{m}$  thicknesses was observed the same less intensive at  $24.98^\circ, 27.5^\circ, 28.8^\circ, 30.1^\circ$ . A peak situated at  $2\theta = 24.98^\circ$  corresponds to a  $d$  spacing of 3.4256  $\text{\AA}$ , which is responsible for the ZnPc molecular macrocycles lying parallel to the plane of the substrate. With further increasing of ZnPc thicknesses (8  $\mu\text{m}$ ) the intensity of reflections at  $2\theta = 11,02^\circ, 16.6^\circ, 17.9^\circ$  became not so pronounced. The intense Bragg's reflection peak broadening positioned at  $2\theta = 6.96^\circ$  after deconvolution shows that ZnPc molecules stand with their long molecular axis nearly perpendicular to the substrate [12].

The XRD results reveal that as-synthesized ZnPc thin films regardless of the thickness have both  $\alpha$ - and  $\beta$ -phases according to the JC-PDS cards No. 21-1986 and 39-1882, respectively. The annealed ZnPc thin films at  $400^\circ\text{C}$ , in hydrogen atmosphere with different thicknesses along with weak peaks show two major

Bragg reflections as shown in Fig. 5. It is observed that the peak broadening situated at  $2\theta = 6.96^\circ$  in the non-annealed films disappear and appear intensive narrow reflections at  $2\theta = 6.99^\circ$  and  $2\theta = 9.3^\circ$ , respectively, which indicate the compression of the ZnPc lattice probably due to thermal relaxation.

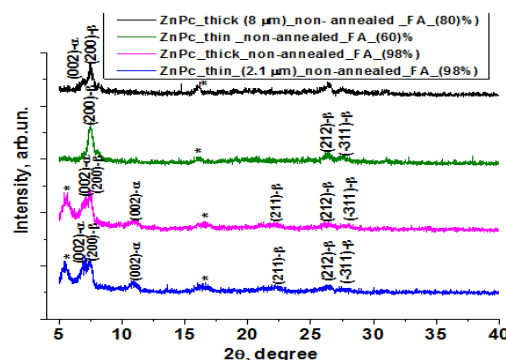


Figure 3: The XRD patterns of ZnPc thin films synthesized on glass substrates from different concentration FA solutions.

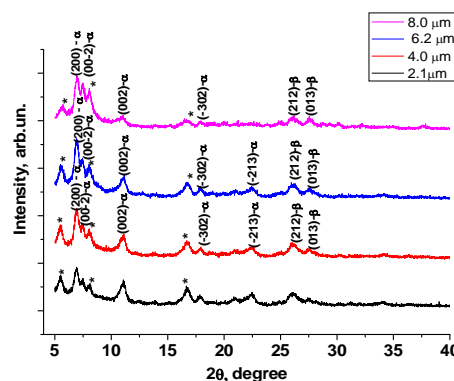


Figure 4: The XRD patterns of ZnPc thin films synthesized on glass substrates from 98% FA solution concentration with different volumes of solution (different film thicknesses).

The XRD patterns of ZnPc film annealed at  $400^\circ\text{C}$  are assigned as  $\beta$ -ZnPc phase and are indexed as for monoclinic crystalline structure [13]. This confirms that the crystallinity of the ZnPc thin films increases on the annealing. FTIR spectra of the non-annealed and annealed at  $400^\circ\text{C}$ , in hydrogen atmosphere of ZnPc thin films are shown in Figure 4. The comparison of them shows that most of the FTIR bands change their position after annealing (see Table I).

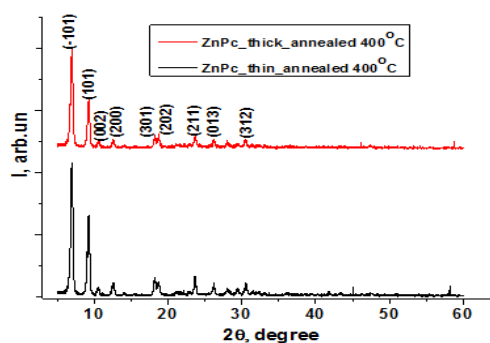


Figure 5: The XRD patterns of annealed ZnPc thin films synthesized on glass substrates from

98% FA solution different volumes of solution (different film thicknesses).

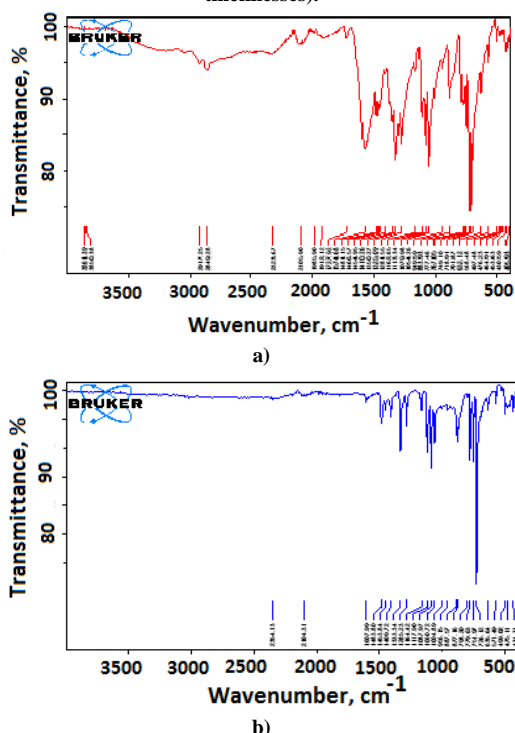


Figure 6: FTIR spectra of 98% FA solution ZnPc thin films of the non-annealed (a) and annealed at 400°C, in hydrogen atmosphere (b).

The bands positioned between 700 and 800  $\text{cm}^{-1}$  for ZnPc in the FTIR spectrum are often used to differentiate between different polymorphs of phthalocyanines and are explained by the assignment of two modes to out-of-plane vibrations and one mode to an in-plane vibration. In our case, as one can see from the Figure 6 (a) the most intensive signal for the non-annealed ZnPc is situated at  $701.8 \text{ cm}^{-1}$ . Sidorov and Terenin [14] had found similar peaks in the spectrum of MgPc after treatment with acetic acid vapor or gaseous HCl. They assigned the changes to an adsorption of a proton to the non-pyrrolic nitrogen atoms and explain as a reduction of the symmetry of the phthalocyanine molecules after complexation. The complexing behavior of ZnPc towards formic acid can be explained by the electron density on the pyrrolic nitrogens. Obviously, a higher  $\pi$ -electron density (ZnPc) will favor the formation of an  $\text{N-H}^+$  bond. The remaining formate ion will then attach itself to the central metal ion. The second intensive signal for non-annealed ZnPc situated at  $883.9 \text{ cm}^{-1}$  indicate the connection of a formate ion to the central metal atom. The third intensive signal positioned at  $1054.2 \text{ cm}^{-1}$  could be assigned to C-H bend. The four signal positioned at  $1574.6 \text{ cm}^{-1}$  is assigned to C=C benzene stretch. The shift of the more intensive third and four bands to lower frequencies by ca.  $6 \text{ cm}^{-1}$  are in agreement with their assignment FTIR (transmission) characteristic vibrations of ZnPc [15].

Non-annealed Wavenumber ( $\text{cm}^{-1}$ )	Assignment	Annealed Wavenumber ( $\text{cm}^{-1}$ )	Assignment
632.1	$\text{C}_\alpha\text{C}_\alpha\text{C}_\beta$ [15]	726.1	Out-of-plane C-H deformation
701.8	$\text{N-H}^+$ bend	751.9	In-plane C-H deformation
749.1	C-H in plane deformation	779.6	Benzene breathing
883.9	Zn-N bend	877.1	Zn-N bend
1054.3	C-H bend	956.1	C-OH
1079.9	In-plane C-H bend	1004.8	C-H bend
1113.3	In-plane C-H bend	1060.7	C-H bend
1162.6	C-H bend	1164.4	C-H bend
1281.5	In-plane C-H bend	1285.2	In-plane C-H bend
1325.1	In-plane pyrrole stretch	1333.3	In-plane pyrrole stretch
1350.3	C-OH	1409.7	Isoindole stretch
1574.6	C=C benzene stretch	1453.8	Isoindole stretch

Table 1  
 Compared wave numbers of the FTIR peaks of ZnPc thin films

The annealing at  $400^\circ\text{C}$  in  $\text{H}_2$  atmosphere do not remove the adsorbed formic acid. The main spectral features, which distinguish between the different crystalline forms of metal substituted family were found to lie in the region  $700\text{-}800 \text{ cm}^{-1}$ . The typical behavior in the spectra with the most intensive signal located at  $726.1 \text{ cm}^{-1}$ , indicate a  $\beta$ -form of ZnPc and is assigned to out-of-plane C-H deformation. Signal positioned at  $751.9 \text{ cm}^{-1}$  could be assigned to in-plane C-H deformation and  $779.6 \text{ cm}^{-1}$  is assigned to benzene breathing in annealed ZnPc film. The  $1004.8$

$\text{cm}^{-1}$ ,  $1060.7 \text{ cm}^{-1}$  and  $1164.4 \text{ cm}^{-1}$  in annealed ZnPc film can be assigned to C-H bend. The signals located at  $1285.2 \text{ cm}^{-1}$  and  $1333.3 \text{ cm}^{-1}$  are assigned to in-plane C-H bend and  $n$ -plane pyrrole stretch, respectively. Peaks at  $1350.3 \text{ cm}^{-1}$  and  $956.1 \text{ cm}^{-1}$  remain unexplained. According to Hanke [16] ZnPc presented modifications of their IR spectra after being exposed to formic acid vapor. Therefore the bands that cannot be found in the spectrum of ZnPc could be assigned to an asymmetrical vibration of  $\text{HCOO}^-$ . In our case the formate ion,  $\text{HCOO}^-$ , displays an

vibration band at  $1350.3\text{ cm}^{-1}$  and an vibration band of a lower intensity around  $956.1\text{ cm}^{-1}$  that correspond to C-OH in-off bending modes. The broadband around  $3000\text{ cm}^{-1}$ -  $3500\text{ cm}^{-1}$  corresponds to O-H stretching vibrations and O-H bending vibrations. After annealing these bands disappear.

So, The XRD and FTIR analysis allow us to conclude that the XRD peaksof ZnPc thin films positioned at  $5.62^\circ$ ,  $7.99^\circ$  and  $16.67^\circ$  from 98% FA solution could be attributed to the Zn(HCOOH)Pc formate supramolecular complexes.

#### 4.2 Optical Properties

The absorbance of ZnPc thin films is shown in Figure 7. The absorbance of ZnPc thin films depend on the film thickness. The highest absorbance for all samples are observed within the UV-Visible region of the solar spectrum with the exception of (430-580) nm region.

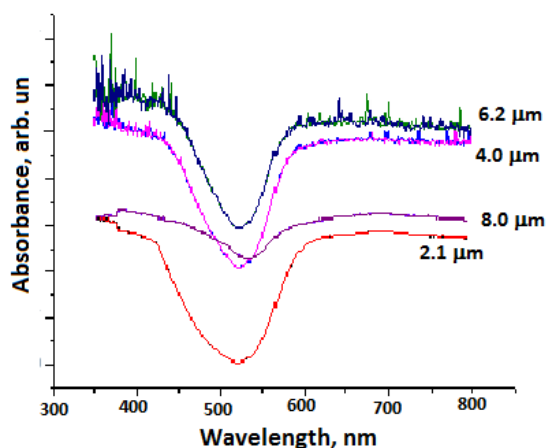


Figure 7: UV-VIS absorption spectra of 98% FA solution ZnPc thin films annealed at  $400^\circ\text{C}$ , in hydrogen atmosphere.

From the absorption spectra the increasing of the absorbance of ZnPc films with further increasing of the thickness are observed. Also, as shift towards the higher wavelength range for the thicker samples is depicted. This shift of spectra indicates the decrease in the optical energy band gap ( $E_g$ ).

#### V. APPLICATION OF ZnPc THIN FILMS IN ORGANIC SOLAR CELLS

The solution-processable Schottky diodesolar cells consists of glass/ITO/PEDOT:PSS/ZnPc( $I_2$ )/Al with different thicknesses of ZnPc layer. Figure 8 shows the configuration of our photovoltaic device. ITO glass substrates with  $4-6\ \Omega/\text{Square}$  were sonicated in acetone, in ethanol and dried under hydrogen flow. Then a  $120\text{ nm}$  thick buffer layer of PEDOT: PSS was spin-coated onto a ITO substrate at  $2500\text{ rpm}$  and subsequently annealed in vacuum at  $150^\circ\text{C}$  for  $30\text{ min}$ . A solution of ZnPc in 98% of FA was made and was dropped on the glass/ITO/PEDOT:PSS substrate. Aluminum electrodes were higher vacuum thermally evaporated. The incident light enters in the device

through transparent ITO side and is absorbed in ZnPc. The absorbed photons result in the creation of bound

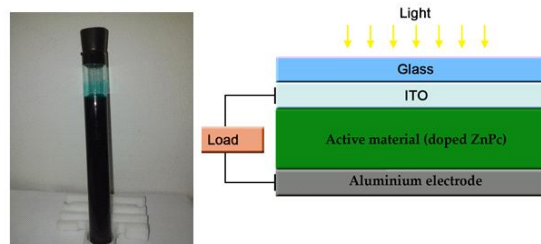


Figure 8: The schematic configuration of solution processable glass/ITO/PEDOT: PSS/ZnPc( $I_2$ )/Al photovoltaic device

electron-holes pairs in the absorbing layer, called excitons. Some of these excitons diffuse to the ZnPc/Al interface where dissociate to electrons and holes. Due to the built-in electric field at the interface, the light-generated holes then move into ZnPc and are ultimately collected at the ITO electrode. This presents a current  $I_{LIGHT}=I_L$ , which, in the presence of a finite external load, makes ITO positively charged with respect to the aluminum electrode, thus forward biasing ( $V_F$ ) the Schottky diode by  $V_F$ . The forward bias causes an injection of holes from ITO to ZnPc and of electrons from aluminum to ZnPc, resulting in a loss current  $I_F$  in a direction opposite to  $I_L$ . The difference  $I_L-I_F$  is the current supplied by the solar cell to the load. When the load is infinite (open-circuit),  $I_L-I_F=0$  and  $V_F=V_{OC}$ =open-circuit voltage. Clearly,  $V_{OC}$  cannot exceed a built-in potential ( $V_{bi}$ ), where  $V_{bi}=\Phi_S-\Phi_M$ .  $\Phi_S$  and  $\Phi_M$  are work functions of the ZnPc organic semiconductor and the metal layer, respectively. In our case  $V_{bi}$  will be the difference between the HOMO energy level of the donor layer (ZnPc) and the work function of the metal (Al). The  $V_{bi}$  values is equal  $1.04\text{ V}$ . The schematic energy diagram of glass/ITO/PEDOT:PSS/ZnPc( $I_2$ )/Al solar cell is shown in Figure 9.

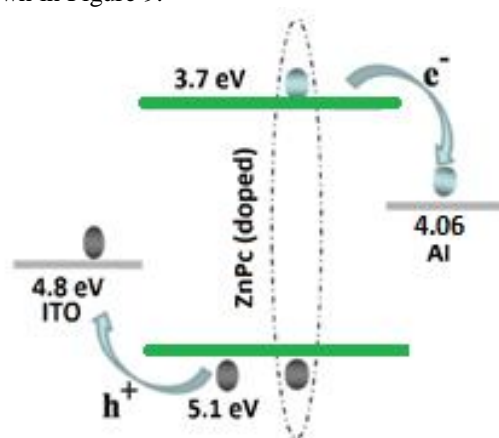


Figure 9: Schematic energy diagram of ZnPc device

The J-V characteristics of the devices were measured by applying a voltage across the device, with positive polarity to ITO and negative polarity to aluminum

(Al). Figure 10 shows the J-V characteristics of the device measured at AM1.5 condition ( $100 \text{ mW/cm}^2$ ), 300 K. The  $V_{OC}$  values of devices with thicknesses of ZnPc  $8.0 \mu\text{m}$  and  $6.2 \mu\text{m}$  from experimental data illustrated in Figure 10 are 1.03V and 0.97 V, respectively. We attribute this high  $V_{OC}$  to: (1) reduced surface states formation, (2) reduced electrode diffusion, and (3) reduced tunneling losses across the interface. J-V curves, also, were analyzed for extracting the photovoltaic parameters: current density ( $J_{sc}$ ), fill factor ( $FF$ ) and efficiency ( $\eta$ ). The photovoltaic parameters for the best devices are presented in Table 2. The obtained values for open circuit voltage and current density are higher than in the case of devices when obtained with thermal vacuum evaporation [17]. The  $FF$  (0.35) and  $\eta$  (0.3%) values calculated are the highest for ZnPc with thickness  $8.0 \mu\text{m}$  (see Table 2). The lower  $V_{OC}$  of devices were observed with thinner layers. The modest value of efficiency was obtained because the FF loss and smaller current density.

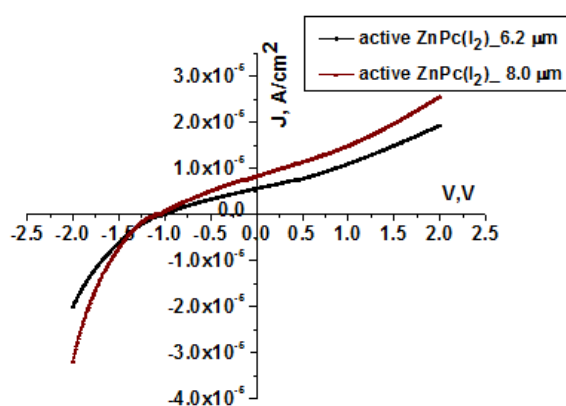


Figure 10: The J-V characteristics of solution processable glass/ITO/PEDOT:PSS/ZnPc ( $I_2$ )/Al photovoltaic device

The parameter	Vacuum evaporation method [17]	Chemical drop casting method, $8.0 \mu\text{m}$ and $6.2 \mu\text{m}$ , respectively	
$V_{OC}$ (V)	0,89	1.03	0.97
$J_{sc}$ ( $\mu\text{A}\cdot\text{cm}^{-2}$ )	2,8	8.2	5.6
$FF$		0.35	0.23
$\eta$ , %		0.3	0.125

Table 2  
 Photovoltaic parameters of the ZnPc( $I_2$ ) devices

According to the theory, the FF is affected by the series and shunt resistances. So, in our case it is rather affected by the higher value of series resistance of the device ( $1.6 \text{ M}\Omega\cdot\text{cm}^2$ ), than value of the shunt resistance ( $4.5 \text{ k}\Omega\cdot\text{cm}^2$ ). We believe, that the modest values of the current density could be attributed to the different recombination mechanisms in the devices.

## CONCLUSION

ZnPc thin films of various thicknesses, ranging from  $2.1 \mu\text{m}$  to  $8.0 \mu\text{m}$  have been prepared from FA solutions of different concentration using the drop casting method. The XRD and FTIR analysis reveal the formation of Zn(HCOOH)Pc formate supramolecular complexes. Also, XRD analysis shows that the as deposited ZnPc films are polycrystalline and contain a mixture of two crystalline phases:  $\alpha$ - and  $\beta$ -. After annealing the improvement of the films crystallinity shown by XRD analysis results in the increasing of the crystallites size from  $20 \text{ nm}$  to  $32 \text{ nm}$  and the presence of the only  $\beta$ - phase. Further on, in this paper we demonstrate the fabrication of Schottky diode solar cells with highest open circuit voltage on the base of optimized technology of ZnPc thin films. Moreover, ITO/PEDOT:PSS/ZnPc( $I_2$ )/Al photovoltaic devices have higher efficiency than the devices obtained with thermal vacuum evaporation method.

## REFERENCES

- [1] K. Wiksne and A. E. Newkirk, "Electrical conductivities of  $\alpha$ - and  $\beta$ -phthalocyanine," Journal of Chemical Physics, 1961, V. 34, pp. 2184–2185.
- [2] S. Senthilarasu, R. Sathyamoorthy, S. Lalitha, A. Subbarayan, K. Natarajan. Thermally evaporated ZnPc thin films—band gap dependence on thickness. Solar Energy Materials and Solar Cells. 2004, Vol. 82, Iss. 1–2, pp. 179–186.
- [3] Shimizu, S., et al. Structurally-modified subphthalocyanines: Molecular design towards realization of expected properties from the electronic structure and structural features of subphthalocyanine. Chem. Commun., 2014, 50, 6949–6966.
- [4] Bezverkhniy V. D. A Short Analysis of Chemical Bonds. Organic Chemistry: Current Research, 2017, V. 6, Iss., pp. 1–18.
- [5] Advanced organic chemistry. Reactions, Mechanisms, and Structure. Third edition. Jerry March, Professor of Chemistry Adelphi University. New York, 1985.
- [6] Kyung Teak Cho, Olga Trukhina, et al. Adv. Molecularly Engineered Phthalocyanines as Hole-Transporting Materials in Perovskite Solar Cells Reaching Power Conversion Efficiency of 17.5%. Energy Mater. 2017, 1601733; DOI: 10.1002/aenm.201601733
- [7] Nyokong, T.; Gasyna, Z., et al. M. J. Phthalocyanine  $\pi$ -cation-radical species: photochemical and electrochemical preparation of [ZnPc(-1)]<sup>+</sup> in solution. Inorg. Chem., 1987, 26, 548.
- [8] Dumoulin F, Durmuş M, Ahsen V, Nyokong T. Synthetic pathways to water-soluble phthalocyanines and close analogs. Coord Chem. Rev. 2010, 254: 2792–2847.
- [9] Hoeben, F. J. M.; Pouderoijen, M. J.; Schenning, A.; Meijer, E. W. Energy transfer in chiral co-assemblies of triple hydrogen-bonded oligo(p-phenylenevinylene)s and porphyrin. Org. Biomol. Chem. 2006, 4, 4460.
- [10] Zorlu Y, Ermeýdan MA, Dumoulin F, Ahsen V, Savoie H, et al. Glycerol and galactose substituted zinc phthalocyanines. Synthesis and photodynamic activity. Photochem Photobiol Sci 8:2009, 312–318.
- [11] Jakob Felix Hitzberger, Claudia Dammann, et al. Making the invisible visible: improved electrospray ion formation of metalloporphyrins/-phthalocyanines by attachment of the formate anion (HCOO<sup>-</sup>). Analyst, 2016, 141, 1347–1355.
- [12] Dhrubojyoti Roy, Nayan M. Das et al. Study of polymorphism of ZnPc LB Thin Film on Annealing. DAE

- Solid State Physics Symposium AIP Conf. Proc.2015, 1731, 030007-1–030007-3; doi: 10.1063/1.4947612
- [13] Chowdhury et al. Studies on phase transformation and molecular orientation in nanostructured zinc phthalocyanine thin films annealed at different temperatures. *Thin Solid Films*, 2012, 520 6695–6704.
- [14] N. Sidorov and I. P. Kotlyar, *Opt. Spektrosc.* 1961, 11, 175, 92
- [15] M. Novotny et al.: The growth of zinc phthalocyanine thin films by pulsed laser deposition *J. Mater. Res.*, 2016, Vol. 31, No. 1, Jan 14,
- [16] W. Hanke and D. Gutschick, *Z. Anorg. Allgem. Chemie*, 1969, 366, 201.
- [17] G.D. Sharma et al. Influence of iodine on the electrical and photoelectrical properties of zinc phthalocyanine thin film devices *Materials Science and Engineering*, 1996, B4I, 222-227.

★ ★ ★